Journal of
Materials Chemistry B

Materials for biology and medicine

Accepted Manuscript

This article can be cited before page numbers have been issued, to do this please use: H. Lin, X. Wang, J. Wu, H. Li and F. Li, *J. Mater. Chem. B*, 2019, DOI: 10.1039/C9TB01455A.

ROYAL SOCIETY OF CHEMISTRY

rsc.li/materials-b

Journal of Materials Chemistry B

View Article Online
DOI: 10.1039/C9TB01455A

COMMUNICATION

Equipment-Free and Visualized Biosensor for Transcription Factor Rapid Assay Based on Dopamine-Functionalized Cellulose Paper†

Received 00th January 20xx,
Accepted 00th January 20xx

DOI: 10.1039/x0xx00000x

www.rsc.org/

Haiyang Lin, Xin Wang, Jiahui Wu, Haiyin Li* and Feng Li*

A cellulose paper-based biosensor has been developed for equipment-free and naked-eye detection of transcription factor (TF) using dopamine as the signal-responsive material based on the Exonuclease III-assisted cycling amplification. Compared with other TFs biosensors, the proposed biosensor enjoyed the low-cost, portable, disposable, and visible features.

Transcription factors (TFs), as DNA-binding proteins, act essential roles in gene expression regulation due to their functions of translating physical/chemical signals into transcriptional changes.[1-3] Meanwhile, more and more evidences have depicted that abnormal expression level in TFs activities are related with many human diseases (cancers, heart disease, diabetes, and so on), and thus, TFs can be regarded as important biomarkers for various diseases evaluating.[4, 5] On the basis of the important role in biomedical field, it is highly desirable to develop simple and convenient assays for TFs accurate and sensitive biosensing. Nevertheless, traditional approaches for TFs detection suffered from the high cost, long operation time, complex operation steps, and some poisonous materials. For the sake of addressing the obstacles above and realizing the exceptional TFs sensing, fluorescence, electrochemistry, surface enhanced resonance Raman scattering, and other techniques have been widely applied in the development of the ideal biosensors.[6-10] For example, Chen et al realized the electrochemical determination of TFs on the basis of the prepared PtNi@MIL-101.[11] Meanwhile, electrochemical biosensor has been also developed by our group for TFs assaying. Despite the high sensitivity and good selectivity, these reported biosensors are still tedious and expensive for the routine analysis of TFs because of the involved labeling/immobilization procedures and large-scale equipments, which necessitate the skilled person manipulating the instruments and assaying the results.[12-14] Moreover, these strategies primarily concentrated on solution system, which is unpractical for their widespread application in analysis of TFs. As a continuation of the work for TFs assaying, we attempt, here, to propose a simple and cost-effective solid strategy for equipment-free and naked-eye detection of TFs.[15, 16]

Cellulose paper-based biosensor (PBs), first reported by Martin, is made up of cellulose paper and signal-responsive material with the low-cost, portable and disposable characteristics.[17-25] These unique advantages make it ideal alternative to other biosensors in the analysis of hydrogen sulfate, moisture and deoxyribonucleic acid.[26-28] However, as far as we are concerned, little information has been done on PBs for TFs biosensing due to the relatively low sensitivity of PBs and low expression level of TFs in biological fluids. Up to now, it is universally acknowledged that the effective approach to improve the sensing performance is to apply high performance materials as signal-responsive elements and take

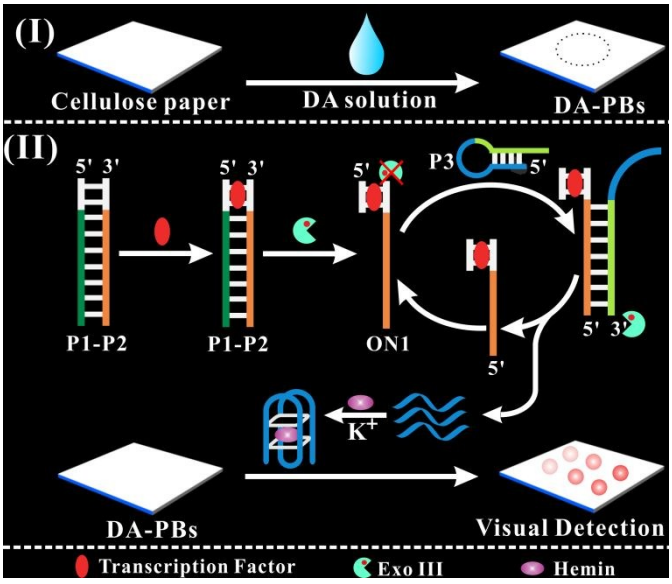

Scheme 1 (I) The fabrication illustration of PBs using dopamine. (II) The mechanism of Exo III-assisted cycling amplification and transduction strategy for TF naked-eye detection based on the fabricated PBs.

College of Chemistry and Pharmaceutical Sciences, Qingdao Agricultural University, Qingdao 266109, PR China
E-mail: lifeng@qau.edu.cn (F. Li); Fax: +86 532 86080855
†Electronic Supplementary Information (ESI) available: experimental sections and additional figures. See DOI: 10.1039/b000000x/

advantage of various tool enzymes.[29-31]

Herein, in this context, dopamine (Fig. S1) with outstanding properties was applied as signal-responsive material in the development of PBs for equipment-free and naked-eye analysis of NF-κB p50, used as the model TF, in the light of the Exo III-mediated cycling amplification. As manifested in Scheme 1, the dopamine-based PBs (DA-PBs) was first prepared through the drop-coating of dopamine on the surface of cellulose paper. In the absence of target NF-κB p50, there were no hemin/G-quadruplexes formation and thus the reaction solution made little influence on the fabricated DA-PBs.[32, 33] As such, DA-PBs maintained the white color unchanged. Upon the addition of NF-κB p50, NF-κB p50@P1-P2 complex generated due to the specific binding sequences in P1-P2 toward NF-κB p50, and protected the 3'-end in P2 against the digestion by Exo III. Subsequently, complex ON1 with ssDNA was released and initiated Exo III-mediated signal transduction/amplification, achieving a strongly efficient 1:N target-recognizable strategy. As expected, large numbers of DNA triggers generated and bound with hemin to produce hemin/G-quadruplexes with the aid of K^+. Due to the catalyzed oxidation of hemin/G-quadruplexes on dopamine, the catalyzed oxidation product (aminochrome, Fig. S2) amount increased accompanied with the decrease of dopamine amount. Thus, the increased aminochrome and decreased dopamine would result in a significant red appearance and enhancement on the surface of DA-PBs, which can be read directly by the naked eyes. On the basis of red variation, equipment-free and naked-eye detection of NF-κB p50 can be readily realized using the fabricated DA-PBs. Overall, the fabricated DA-PBs is low-cost, portable, disposable, and visible by naked eyes compared with solution-phase biosensors, and displays a significant prospect for point-of-care diagnosis at home or in remote developing world locations.

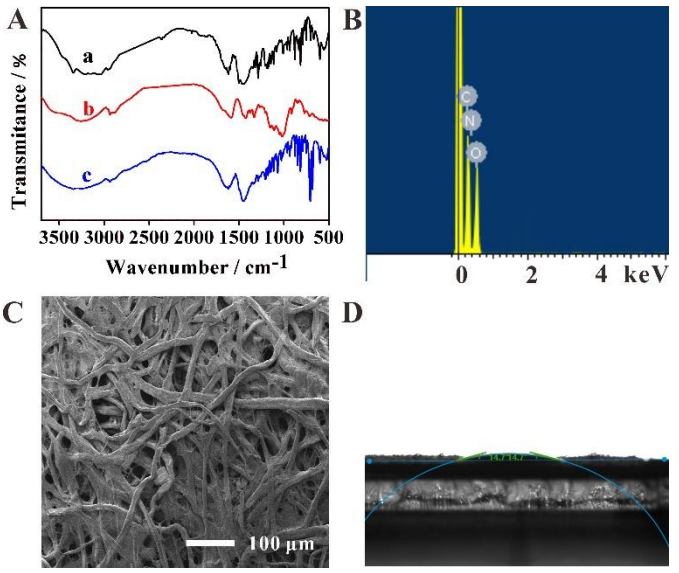

Fig. 1 (A) FT-IR spectra of (a) dopamine, (b) cellulose paper, and (c) DA-PBs. (B) Energy dispersive spectroscopy of DA-PBs. (C) SEM image of DA-PBs. (D) Contact angle of DA-PBs.

To guarantee the effective response of the fabricated DA-PBs toward NF-κB p50, dopamine must be attached to the cellulose paper. Fourier transform infrared (FT-IR) spectrum of DA-PBs in Fig. 1A displays obvious characteristic peaks (1446 cm^{-1}, 1206 cm^{-1}, 802 cm^{-1}) corresponding to dopamine compared with that of cellulose paper alone, implying that dopamine has been prosperously anchored on the paper's surface. Meanwhile, in Fig. 1B and Fig. S3A, it can be observed that DA-PBs presents a new signal located at 0.39 KeV, which is attributable to N element undoubtedly deriving from dopamine. Very interestingly, the fabricated DA-PBs possesses the same three-dimensional network structure and hydrophilicity with that of cellulose paper (Fig. 1C and D, Fig. S3B, and C), making for the occurrence of recognizable reactions between dopamine and target analytes, and the improvement of sensing performance.

Further, the fabricated DA-PBs was implemented in the analysis of target NF-κB p50 based on the Exo III-mediated cycling amplification reaction. Gel electrophoresis technique was first conducted to justify the feasibility of the NF-κB p50-initiated signal amplification with the assistance of Exo III. It can be clear seen from Fig. 2A that P1-P2 duplex and hairpin DNA P3 displayed narrow bands without other structures, respectively. When reacted with Exo III, P1-P2 duplex exhibited no band signal, implying the fact that P1-P2 was completely digested by Exo III. However, upon the addition of NF-κB p50, new band located at the longer distance than that of P1-P2 duplex appeared and was due to the complex ON1, revealing the specific response of P1-P2 duplex toward NF-κB p50 and effective protection of P2 against Exo III-mediated digestion. Meanwhile, the system comprising of P1-P2 duplex, P3 hairpin, and Exo III, just demonstrated the band of P3, suggesting the complete digestion of P1-P2 duplex too and the untransformed configuration of P3. The system comprising of P1-P2 duplex, P3 hairpin, NF-κB p50, and Exo III, displayed new band at the foremost location, attributable to the DNA triggers that can bind with hemin to generate hemin/G-quadruplex.

The response of DA-PBs toward NF-κB p50 was also investigated through the color change. In the absence of NF-κB p50, image (a) in Fig. 2B gives the same white signal with that of control sample. Once the target NF-κB p50 was added, red signal was observed from the images. It came as no surprise to us that hemin/G-quadruplexes generated via the target NF-κB p50-initated cycling amplification reaction, and the generated hemin/G-quadruplexes can consume dopamine and transform them into aminochrome, accompanied with the appearance of red signal. Interestingly, the red signal enhanced with the increase of NF-κB p50 amount, which is consistent with the sensing principle that more NF-κB p50 would initiated more Exo III-mediated digestion reaction to generate more hemin/G-quadruplexes, subsequently contributing to the formation of more aminochrome. The further verification of the proposed strategy in solution was manifested in Fig. S4. In addition, changing the sequences in P1-P2, the proposed solid sensor or solution sensing system displayed very weak signal (Fig. S5), firmly verifying the critical role of the sequences in

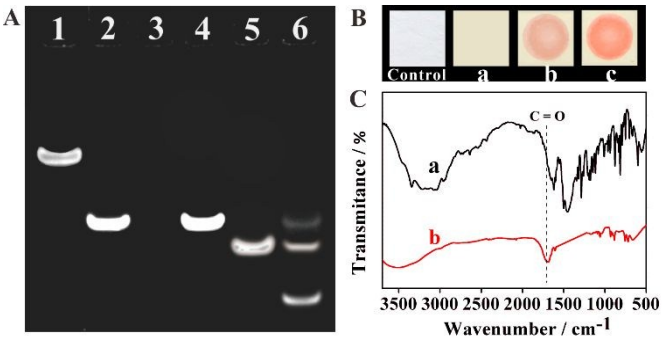

Fig. 2 (A) Nondenaturing PAGE images of (1) P1-P2, (2) P3, (3) P1-P2 + Exo III, (4)P1-P2 +P3+ Exo III , (5) P1-P2 + NF-κB p50 + Exo III , (6) P1-P2 +P3+ NF-κB p50 + Exo III. (B) The images of DA-PBs: (a) 0 nM NF-κB p50, (b) 300 nM NF-κB p50, (c) 1500 nM NF-κB p50 . (C) FT-IR spectra of different samples: (a) dopamine, and (b) dopamine + NF-κB p50.

P1-P2 for developing sensor for NF-κB p50 assay. To confirm the effective recognition of DA-PBs by NF-κB p50, FT-IR characterizations were also conducted (Fig. 2C). Through the target-initiated catalyzed oxidation reaction, the sample (b) presented new peak located at 1690 cm^{-1}, which was ascribed to the carbonyl originating from the catalyzed oxidation product aminochrome. As a consequence, it is completely feasible to realize the equipment-free and naked-eye detection of NF-κB p50 by coupling the fabricated DA-PBs and Exo III-mediated signal transduction/amplification strategy.

To evaluate the sensing performance of the fabricated DA-PBs to detect target NF-κB p50, an array of samples containing NF-κB p50 with different concentrations were measured. Fig. 3 gives the resulting color response of the fabricated DA-PBs subjected to various NF-κB p50 amounts under different incubation time. Very interestingly, the color response is rapid with the time of only 20 s, benefitting the rapid, in-situ, and on-site detection. It is not favorable for the red signal enhancement when incubation time was extended to 30 s. Meanwhile, upon the treatment of DA-PBs with elevating NF-κB p50 amounts, more dopamine was catalyzed oxidation into aminochrome and a gradual enhancement in the red signal was determined, which was assigned to the formation of abundant hemin/G-quadruplexes and their excellent catalyzed oxidation ability. More importantly, the appeared red signal can be seen directly by the naked eyes, and the signal change can be readily comprehended by unprofessional people, making for the great potential application in remote developing world locations. From the weakest red signal read directly by the naked eyes, the minimum concentration for NF-κB p50 was determined to be 40 nM, which is higher than that of the proposed strategy in solution system and other existing methods (Table S2，Fig. S6), but fulfils the requirements of analysis of NF-κB p50 in biological samples. Furthermore, three differently fabricated DA-PBs were applied in detection of NF-κB p50, respectively, and the information indicated that the output signals are about the same with each other, justifying the excellent reproducibility of the fabricated DA-PBs (Fig. S7). In addition, the proposed DA-PBs enjoys the advantages of low cost,

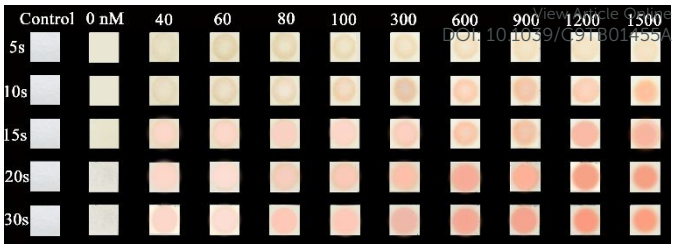

Fig. 3 The color responses of DA-PBs to various NF-κB p50 concentrations under different reaction time.

portable, disposable, andvisualization, and thus, is more practical than solution-phase biosensor.

It is well known that an ideal biosensor not only enjoys high sensitivity but also possesses excellent selectivity, and thus, the specific recognition of the prepared DA-PBs to NF-κB p50 against other proteins was investigated. Insulin, C-Jun, and BSA were applied as the interfering biomolecules to conduct the experiment (Fig. 4A). Among them, insulin and C-Jun can bind with the special DNA sequences, which are different from the sequences recognized by NF-κB p50. Obviously, all images of three interfering proteins depicted white color signal, which is about the same with that of the control sample. Contrarily, the image of NF-κB p50 manifested evident red signal. Similar signal variation can be also obtained from the measurement in solution system (Fig. S8A). Meanwhile, these interfering proteins made little influence on the diagnosis result. These changed signals firmly justified that the fabricated DA-PBs can effectively recognize target NF-κB p50 against other proteins.

Besides the sensitivity and selectivity, stability is also a significant parameter for the developed biosensor. To assess DA-PBs's stability toward NF-κB p50, we lay up the fabricated DA-PBs in the fridge (4 °C) for 7.0 days and subsequently test its responsive ability (Fig. 4B). In the absence of target NF-κB p50, the image is identical with that of control sample, which stated the ascendant stability of DA-PBs, profiting the potential practical application. FT-IR spectra were employed to further corroborate the viewpoint (Fig. S8B). Noticeably, Slight change in FT-IR peaks of the stored DA-PBs was observed. After that, the treated DA-PBs was subjected to different NF-κB p50 amounts. The DA-PBs displayed the gradually increased red signal along with the elevating NF-κB p50 concentrations. Moreover, the red signal of DA-PBs under each NF-κB p50 concentration is as large as that of the untreated DA-PBs. Thus, there is no denying that the fabricated DA-PBs exhibited sufficient stability for equipment-free and naked-eye detection of NF-κB p50 after storing for a period.

Taking account of the wonderful properties of DA-PBs, it was expected to assay NF-κB p50 in biological samples. In the present study, the sample was fabricated via the 3:7 volume mixing of serum and Tris-HCl buffer. Prior to analysis, the biological sample was determined by the Elisa method, and the results demonstrated that no NF-κB p50 existed in the proposed sample. As expected, through the treatment of the sample, the DA-PBs maintained the white color unchanged compared with the control sample, justifying the strong interfering ability of

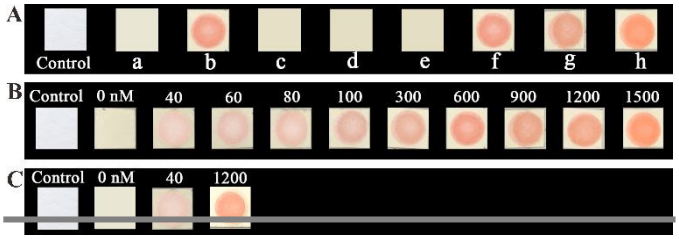

Fig. 4 (A) The images of DA-PBs under different conditions: control sample: DA-PBs; (a) in the absence of the proteins; (b) NF-κB p50; (c) Insulin; (d) C-Jun; (e) BSA; (f) NF-κB p50 + Insulin; (g) NF-κB p50 + C-Jun; (h) NF-κB p50 + BSA. Their concentrations were 1500 nM. (B) The images of DA-PBs under different conditions. (C) The images of DA-PBs correspond to different amount of.NF-κB p50 in human sample.

DA-PBs on the substances that may existed in biological matrixes. Further, NF-κB p50 with the amount of 40 and 1200 nM was spiked into the sample, respectively, and the resulting samples were detected using the fabricated DA-PBs. As shown in Fig. 4C, distinct red signal was observed and strengthened with the increase of NF-κB p50 amounts, clearly illustrating the significant potential of DA-PBs for NF-κB p50 biosensing in biological matrixes.

In conclusion, we have proposed a novel paper-based biosensor (DA-PBs) for equipment-free and naked-eye analysis of NF-κB p50 through using dopamine as the signal-responsive material based on the Exo III-mediated cycling amplification reaction. In the presence of target NF-κB p50, it experienced dopamine consumption and aminochrome production correlated with the red signal increase due to the different color of them by virtue of hemin/G-quadruplex-catalyzed oxidation of dopamine. As a consequence, the fabricated DA-PBs readily serves as a powerful solid biosensor for NF-κB p50 biosensing, with the advantages of low cost, visualization, portable and disposable characteristics, as compared to solution-phase biosensor. Featured with these merits, the developed DA-PBs was prosperously applied in the analysis of NF-κB p50 in biological matrix. Furthermore, the DA-PBs can also be readily applied in the analysis of other biomolecules through simply changing the target recognition DNA structure, thus offering a versatile paper-based biosensor for equipment-free and naked-eye detection of various biomolecules. Consequently, the fabricated DA-PBs has a great prospect for point-of-care diagnosis in remote developing world locations.

This work was financially supported by National Natural Science Foundation of China (21605093 and 21775082), and the Special Foundation for Distinguished Taishan Scholar of Shandong Province (ts201511052).

Conflicts of interest

There are no conflicts of interest to declare.

Notes and references

1 P. Brennan, R. Donev and S. Hewamana, *Mol. Biosyst.*, 2008, **4**, 909−919.
2 A. Papantonis and P. R. Cook, *Chem. Rev.*, 2013, **113**, 8683−8705.
3 E. Pazos, A. Jiménez-Balsa, J. Mascareñas and M. E. Vázquez, *Chem. Sci.*, 2011, **2**, 1984−1987.
4 K. L. Ai, B. H. Zhang and L. H. Lu, *Angew. Chem. Int. Ed.*, 2009, **48**, 304−308.
5 M. Chakraborty and S. Roy, *Chem. Commun.*, 2016, **53**, 376−379.
6 J. J. Zhang, W. T. Wang, S. H. Chen, Y. Ruo, X. Zhong and X. P. Wu, *Biosens. Bioelectron.*, 2014, **57**, 71−76.
7 L. J. Xu, Z. C. Lei, J. Li, C. Zong, C. J. Yang and B. Ren, *J. Am. Chem. Soc.*, 2015, **137**, 5149−5154.
8 C. Li, Y. Q. Tao, Y. Yang, Y. Xiang and G. X. Li, *Anal. Chem.*, 2017, **89**, 5003−5007.
9 J. F. Chang, X. Wang, J. Wang, H. Y. Li and F. Li, *Anal. Chem.*, 2019, **91**, 3604−3610.
10 X. M. Shi, G. C. Fan, X. Tang, Q. Shen and J. J. Zhu, *Biosens. Bioelectron.*, 2018, **109**, 190−196.
11 H. Yu, W. Zhang, S. C. Lv, J. Han, G. Xie and S. P. Chen, *Chem. Commun.* , 2018, **54**, 11901−11904.
12 A. Vallee-Belisle, A. J. Bonham, N. O. Reich, F. Ricci and K. W. Plaxco, *J. Am. Chem. Soc.*, 2011, **133**, 13836−13839.
13 D. S. Zhu, L. Wang, X. W. Xu and W. Jiang, *Biosens. Bioelectron.*, 2016, **75**, 155−160.
14 Y. Zhang, F. Ma, B. Tang and C. Y. Zhang, *Chem. Commun.* , 2016, **52**, 4739−4748.
15 W. L. Wei, L. Wu, C. Xu, J. S. Ren and X. G. Qu, *Chem. Sci.*, 2013, **4**, 1156−1162.
16 R. N. Jia, W. G. Tian, H. T. Bai, J. M. Zhang, S. Wang and J. Zhang, *Nat. Commun.*, 2019, **10**, 795.
17 C. Parolo and A. Merkoci, *Chem. Soc. Rev.*, 2013, **42**, 450−457.
18 P Wang, M. Y. Wang, F. Y. Zhou, G. H. Yang, L. L. Qu and X. L. Miao, *Electrochem.Commun.*, 2017, **81**, 74−78.
19 G. I. Salentijn, M. Grajewski and E. Verpoorte, *Anal. Chem.*, 2018, **90**, 13815−13825.
20 S. Kim, E. Jung, M. J. Kim, A. Pyo, T. Palani, M. S. Eom, M. S. Han and S. Lee, *Chem. Commun.* , 2012, **48**, 8751−8753.
21 S. V. Costa, A. S. Goncalves, M. A. Zaguete, T. Mazon and A. F. Nogueira, *Chem. Commun.*, 2013, **49**, 8096−8098.
22 M. Ikeda, K. Fukuda, T. Tanida, T. Yoshii and I. Hamachi, *Chem. Commun.* , 2012, **48**, 2716−2718.
23 M. I. Khazi, W. Jeong and J. M. Kim, *Adv. Mater.*, 2018, **30**, 1705310.
24 T. Gorai and U. Maitra, *J. Mater. Chem. B.*, 2018, **6**, 2143−2150.
25 J. Credou and T. Berthelot, *J. Mater. Chem. B.*, 2014, **2**, 4767−4788.
26 J. Rull-Barrull, M. d'Halluin, E. Le Grognec and F. X. Felpin, *Chem. Commun.* , 2016, **52**, 2525−2528.
27 D. K. Ye, L. Li, Z. H. Li, Y. Y. Zhang, M. Li, J. Y. Shi, L. H. Wang, C. H. Fan, J. H. Yu and X. L. Zuo, *Nano. Lett.*, 2019, **19**, 369−374.
28 F. Guder, A. Ainla, J. Redston, B. Mosadegh, A. Glavan, T. J. Martin and G. M. Whitesides, *Angew. Chem. Int. Ed.* , 2016, **55**, 5727−5732.
29 X. M. Qu, D. Zhu, G. B. Yao, S. Su, J. Chao, H. J. Liu, X. L. Zuo, L. H. Wang, J. Y. Shi, L. H. Wang, W. Huang, H. Pei and C. H. Fan, *Angew. Chem. Int. Ed.* , 2017, **56**, 1855−1858.
30 H. Y. Li, C. F. Wang, T. Hou and F. Li, *Anal. Chem.*, 2017, **89**, 9100−9107.
31 H. Y. Li, J. F. Chang, P. P. Gai and F. Li, *ACS. Appl. Mater. Interfaces.*, 2018, **10**, 4561−4568.
32 H. B. Albada, E. Golub and I. Willner, *Chem. Sci.*, 2016, **7**, 3092−3101.
33 T. Tian, Y. Q. Chen, S. R. Wang and X. Zhou, *Chem.*, 2018, **4**, 1314−1344.

View Article Online
DOI: 10.1039/C9TB01455A

View Article Online
DOI: 10.1039/C9TB01455A

Graphical Abstract

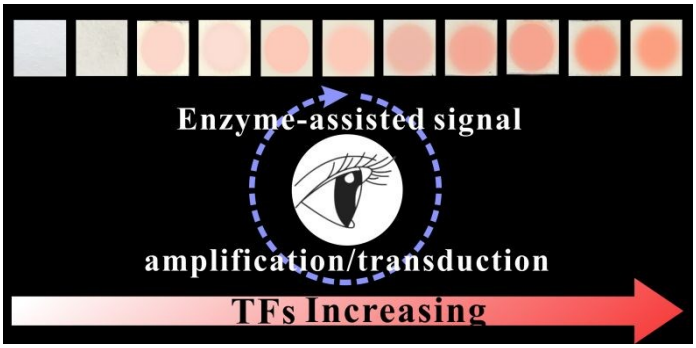

Dopamine-functionalized cellulose paper with low cost, portable, and disposable features was applied for equipment-free and naked-eye detection of transduction factor based on the enzyme-assisted signal amplification/transduction reaction.